Received: 6 June 2019 | Revised: 4 July 2019 | Accepted: 16 July 2019

DOI: 10.1002/ppap.201900122

FULL PAPER

PLASMA PROCESSES AND POLYMERS

Ceramide cross-linking leads to pore formation: Potential mechanism behind CAP enhancement of transdermal drug delivery

Jonas Van der Paal[1] | **Gregory Fridman**[2] | **Annemie Bogaerts**[1]

[1]Research Group PLASMANT, Department of Chemistry, University of Antwerp, Wilrijk, Belgium

[2]C & J Nyheim Plasma Institute, Drexel University, Camden, New Jersey

Correspondence
Jonas Van der Paal, Research Group PLASMANT, Department of Chemistry, University of Antwerp, Wilrijk, Belgium.
Email: jonas.vanderpaal@uantwerpen.be

Funding information
Fonds Wetenschappelijk Onderzoek, Grant/Award Number: 11U5416N

Abstract

In recent years, cold atmospheric plasma (CAP) has been proposed as a novel method to enhance transdermal drug delivery, while avoiding tissue damage. However, the underlying mechanism for the increasing skin permeability upon CAP treatment is still undefined. We propose a mechanism in which CAP-generated reactive species induce cross-linking of skin lipids, leading to the generation of nanopores, thereby facilitating the permeation of drug molecules. Molecular dynamics simulations more, our results indicate that to achieve maximum enhancement of the permeability, the optimal treatment will depend on the exact lipid composition of the skin, as well as on the CAP source used.

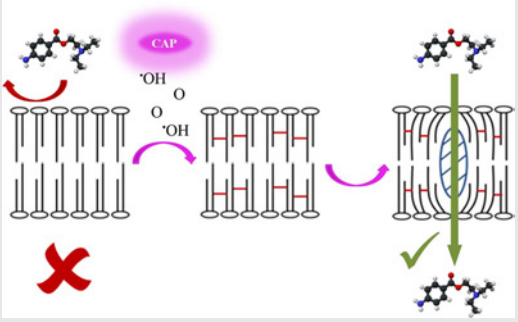

KEYWORDS

ceramides, molecular dynamics, plasma-initiated polymerization, stratum corneum, transdermal drug delivery

1 | INTRODUCTION

Transdermal drug delivery (TDD) is an innovative and very attractive drug administration method, as it possesses many advantages over other administration methods, including, for example, avoiding the first-pass effect of the liver, reducing side effects, and the ease of application of the drug.[1] Nowadays, TDD systems are already being used in the treatment of a variety of diseases, for example, to deliver chemotherapeutics.[2] One of the main challenges of TDD, however, is that very few drugs can be administered transdermally. Indeed, to achieve an effective concentration of the applied drug in the body, there are very strict limitations to the molecular weight and lipophilicity of the drug molecule.[3] Therefore, TDD is nowadays combined with systems that enhance the permeability of the skin, either mechanically or chemically. However, until now, all these enhancement techniques struggle with the balance of enhancing the delivery of drugs to achieve a biologically active level, while avoiding side effects, such as deeper tissue damage in the process.[4] The challenge of getting drugs through the skin tissue and into the blood vessels is a function of (a) the chemical composition of the drug, as well as (b) the skin structure.

When focusing on the skin structure, research has shown that the outermost layer of the skin, that is, the stratum corneum (SC), forms the greatest barrier for the transdermal delivery of drugs.[3,4] Various studies revealed that the structure of the SC, being only a few

hundred micron thick, mainly contains stacked bilayers of fully extended ceramides (i.e., six main ones, CER (1–6) that differ from each other mainly by the head group), cholesterol, and free fatty acids.[5–7] It is reported that permeation through the SC does not significantly depend on biological processes, but rather is more of a passive diffusion process, as the TDD rate for in vitro studies is roughly the same as for in vivo human trials.[8] Recently, cold atmospheric plasma (CAP), that is, an ionized gas that contains a cocktail of reactive species, has been demonstrated to enhance the transdermal uptake of drugs in a very gentle way, that is, while avoiding side effects such as deeper tissue damage.[9–13]

In search of an explanation behind this plasma-induced increase in permeability of the SC, we suggest a reversible pore formation mechanism, as illustrated in Figure 1.

In this process, lipid oxidation due to CAP-generated reactive oxygen species (ROS; e.g., $^{\bullet}O$ or $^{\bullet}OH$ radicals) leads to the creation of cross-linkages between lipids (such as ceramides) present in the SC. Two possible mechanisms leading to the cross-linking of neighboring ceramides can be identified. A first option is that cross-linking occurs due to a process called lipid peroxidation, which starts by the abstraction of an allylic hydrogen due to impinging CAP-generated radicals (e.g., $^{\bullet}O$ or $^{\bullet}OH$), followed by O_2 addition and the formation of an O–O bridge.[14,15] A second option is a polymerization process that does not involve the formation of an O–O bridge, in which the allylic carbon radical created after H-abstraction immediately reacts with the double bond of a neighboring ceramide (cf. free radical polymerization of alkenes). Either way, due to these cross-linkages, nanopores are generated in the SC structure, which will facilitate the passive diffusion of drug molecules through skin tissue. Since (a) these are nanoscale restructurings of the SC structure, and (b) the SC is continuously regenerated, the barrier function of the skin can easily be restored.

This hypothesis is based on observations made by multiple other researchers. First of all, the process of lipid oxidation in the presence of ROS had been demonstrated extensively in literature.[14,16,17] As CAPs contain a variety of ROS, it is only logical to assume that oxidation of skin lipids is involved in the underlying mechanism of CAP-assisted TDD. Next, it has been shown by Melo et al.[18] that ceramides containing saturated lipid tails are not oxidized when applying oxidative stress. This suggests that if CAP-generated ROS reach the skin lipids, they can only react with unsaturated lipid tails. In this case, cross-linking of these tails, which have the same structure as the aliphatic tail of free fatty acids, is very likely to occur, as has already been demonstrated by multiple researchers.[19–22]

In this paper, we explore the validity of the proposed reversible pore formation mechanism by employing molecular dynamics (MD) simulations. By comparing bilayer systems containing different numbers of cross-linked (CL) lipids, we test if this process can explain the increase in permeability of the SC. Such MD simulations can give us molecular level insight in the effect of CL ceramides. Indeed, this type of simulations has already been applied successfully to examine the dynamic and structural behavior of lipid structures under oxidative stress.[23–25]

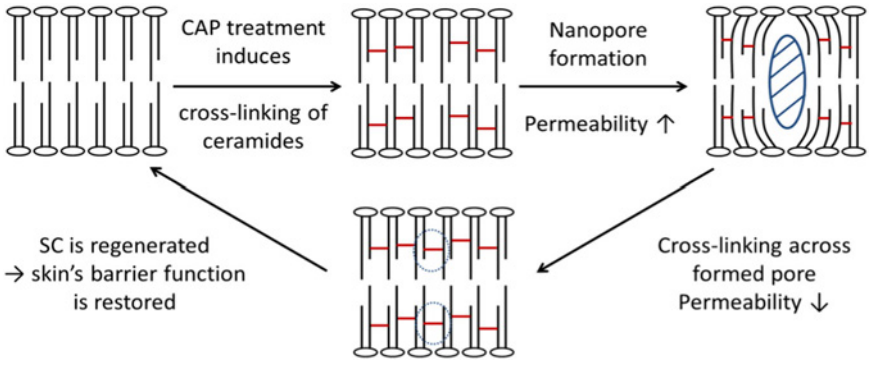

FIGURE 1 Proposed mechanism of plasma-induced reversible pore formation in the SC. Reactive oxygen species present in cold plasma induce lipid oxidation in the unsaturated lipid tails of the ceramides in the SC. This leads to the formation of cross-linkages between neighboring lipids. The formation of oligomers of ceramides leads to the generation of voids in between different oligomers. This will enhance the permeability of the SC. Upon prolonged CAP treatment, the entire system will eventually be cross-linked (on a local scale), which will suppress the initial increase of the SC's permeability. As this process only occurs on a nanoscale, the continuous regeneration of the skin will ensure that no prolonged damage occurs. CAP, cold atmospheric plasma; SC, stratum corneum

2 | COMPUTATIONAL DETAILS

As a model system for the SC, we mimic its structure by a ceramide bilayer, ignoring the presence of free fatty acids and cholesterol. This approach can be justified as ceramides are considered to be the most important determinant of the barrier function of the skin.[26] All simulated systems contain, in total, 1,800 ceramides, surrounded by 72,000 water molecules on each side. The initial structure was created using the Packmol program[27] and an energy minimization is performed, after which we performed a 900 ns simulation, employing a time step of 30 fs. This proved to be enough to equilibrate the structures, based on an analysis of the *x*-, *y*-, and *z*-dimensions of the system, as well as the total potential energy of the system. The last 250 ns of this run were used to collect the data shown in the figures below. The systems were simulated in the NPT ensemble, using Bussi's velocity rescaling thermostat[28] (at 310 K) and the Parrinello–Rahman barostat[29] (at 1 atmosphere). The nonreactive, coarse-grained Martini force field was used in these simulations.[30] In a coarse-grained force field, multiple atoms are grouped into one bead, thereby reducing the number of particles used to represent each lipid. This allows us to simulate far bigger systems compared to what is possible with all-atom or united-atom force fields. Moreover, since nonreactive force fields do not allow existing bonds to be broken or new bonds to be created during a simulation, cross-linkages between different ceramides were defined in the initial structures. This nonreactive approach was chosen as it allows to simulate longer time scales, as well as bigger length scales in comparison to the reactive counterpart,[31] and this is necessary to study the abovementioned hypothesis of cross-linking and pore formation. CL ceramides were added to the force field by including the required topology files (see Appendix A). To construct the topology file of a ceramide dimer, a bond was added between neighboring beads, applying the same bond length and force constant present between other beads of the same types (C1 and C3 beads, see Marrink et al.[30] for more information). The description of the additional angles, created by this new bond, was based on angles between identical beads as well. To construct oligomers containing more ceramides, the same approach was followed.

As mentioned in the introduction, two possible mechanisms leading to the cross-linking of ceramides can be identified. As the exact mechanism is unknown, we opted to implement a hybrid structure in our MD simulations. Indeed, although the lipid peroxidation mechanism involving an O–O bridge between ceramides is the most straightforward (as a free radical polymerization process is sterically hindered due to the large ceramide tails), this does require an additional step, and therefore the presence of O_2. If it would be only lipid peroxidation, a polar Martini bead would need to be introduced in between the CL ceramides, to account for the O–O bridge. However, if it would only be a free radical polymerization process, the double bonds would be lost during the reaction while the ceramide structures remain apolar. In the hybrid structure used in our simulations, the bead representing the double bond is preserved (cf. lipid peroxidation mechanism), but no polar bead is implemented in the structure (cf. the free radical polymerization mechanism), as is illustrated in Figure 2. Furthermore, as we are mainly interested in the effect of cross-linking ceramides on the overall membrane structure, regardless of the exact configuration of the polymerized chains, this hybrid structure is adequate to provide this information.

To investigate the effect of different cross-linking degrees, we constructed multiple systems, which contain 0, 400, 800, 1,200, or 1,600 CL ceramides, corresponding to a cross-linking degree of 0%, 22%, 44%, 66%, or 88%. These values were chosen to scan the entire range of CL fractions, which can experimentally be achieved by

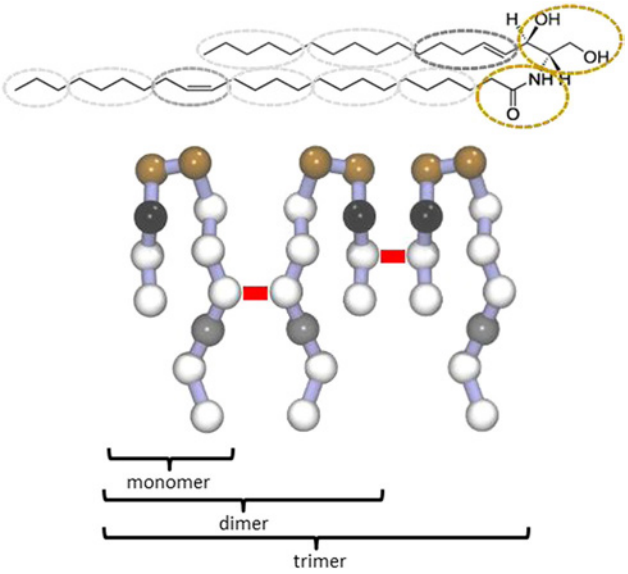

FIGURE 2 The top figure shows the all-atom representation of one native ceramide, whereas the bottom figure illustrates the Martini-interpretation of the same ceramide in trimer configuration (one monomer is one native ceramide; the same colors are used for the ovals (group of atoms) in the top figure and corresponding beads in the bottom figure; see text). Moreover, the bottom figure schematically illustrates how the cross-linked structures are built for the simulations. The longer chains (5-, 10-, and 20-linked) are built in the same way. The color (and thus the type) of each bead is based on the polarity of the corresponding group of atoms which the bead represents

varying the duration of plasma treatment. Moreover, the effect of chain length of CL ceramides was investigated as well (hereafter referred to as the degree of polymerization [DOP]), that is, we built structures with polymerized ceramide chains containing 5, 10, or 20 ceramides (DOP = 5, 10, or 20). We opted to focus on these longer polymerized chains (instead of, e.g., dimers or trimers), because the polymerization process is a chain reaction. This means that it is more likely to generate one long chain instead of multiple short chains (as in the latter case, multiple radicals are needed to start each polymerization process). The idea of the polymerized or CL ceramide chains is illustrated in Figure 2.

The analysis was performed using a search and find algorithm, which calculates the void size in each system.[32] In a first step, the entire system was divided into cubic cells, with dimensions of $2.5 \times 2.5 \times 2.5$ Å^3. Next, the system was scanned for free cells, that is, cells which do not contain any atoms. Afterward, the volume of all free cells was summed up to get the total void size mentioned in the figures below. However, when calculating this void size, we only used larger clusters of cells, that is, clusters that contained at least 15 linked free cells. Using this boundary condition, we ignored very small voids between neighboring lipids, because these would have no effect on the permeability of larger drug molecules. The graphs shown below illustrate the relative increase in void size, which is calculated as follows:

$$\Delta_{\text{Void size}} = \frac{\text{Void size}_{\text{CL}} - \text{Void size}_{\text{N}}}{\text{Void size}_{\text{N}}} \times 100\%.$$

With $\Delta_{\text{Void size}}$ being the relative increase in void size, Void size$_{\text{CL}}$ is the total void size in a system that contains CL ceramides, and Void size$_{\text{N}}$ is the free void size in the native system, that is, the system containing only monomeric ceramides.

To determine the average void size and the associated error bars, 50 snapshots were selected from the last 250 ns of each simulation (i.e., one every 5 ns). Furthermore, all systems were run in duplicate (starting from different lateral distributions of the lipids in the input geometry). The free void size was calculated for each individual snapshot, which renders a total of 100 values for all data points shown in the figures below.

3 | RESULTS AND DISCUSSION

Figure 3 illustrates the calculated relative increase in void size for different cross-linking degrees and different

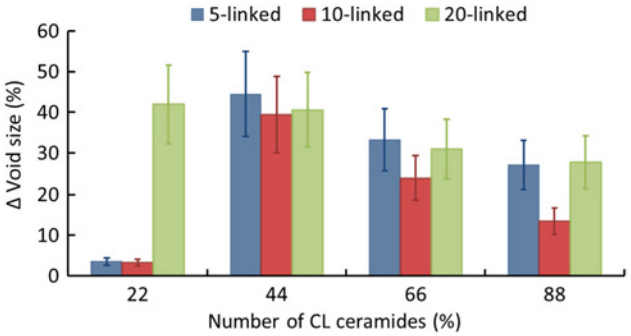

FIGURE 3 Effect of the cross-linking fraction and DOP on the relative increase in total void size with respect to the system without cross-linking. Upon increasing the CL fraction of the system, the free void size first increases (up to CL fractions of 44%), after which the total free void size decreases again. The DOP does not have a big effect on this trend. CL, cross-linked; DOP, degree of polymerization

DOP. Upon increasing the cross-linking degree of the ceramides present in the SC structure up to 44%, the total void size increases drastically. The relative increase in void size, compared with a structure containing only monomeric ceramides, reaches about 40% for all DOPs investigated. However, when increasing the number of CL ceramides even further, the relative increase in void size decreases again. Although the graphs show similar trends for all DOPs, the exact value of this threshold depends on the length of the polymerized ceramide chain. Indeed, for a DOP of 20, there is already a significant effect on the void size for a CL degree of 22%, whereas for DOPs of 5 or 10, the effect is only significant for a CL fraction of 44%.

In terms of application for TDD, these results indicate that the enhancement of the permeability of the SC by CAP will strongly depend on the treatment time. During treatment, the permeability of the SC will increase, reaching maximum enhancement for a certain treatment time. Prolonged treatment will have the opposite effect, suppressing the further increase in permeability. The optimal treatment time will be determined by the composition of the SC (patient specific) as well as the CAP source used.

It has to be acknowledged that the error bars shown in Figure 3 are quite large (~20% of the average value). However, performing additional simulations or increasing the sampling time period did not reduce these error bars. This is due to the combination of (a) the dynamic nature of the lipids in the bilayer and (b) the analysis tool used in this study. Indeed, the flexible lipid tails can easily cross through one of the cells that is part of a bigger cluster, due to which the cluster could be broken into two smaller parts, which separately would not be included in the calculations anymore (see above). This

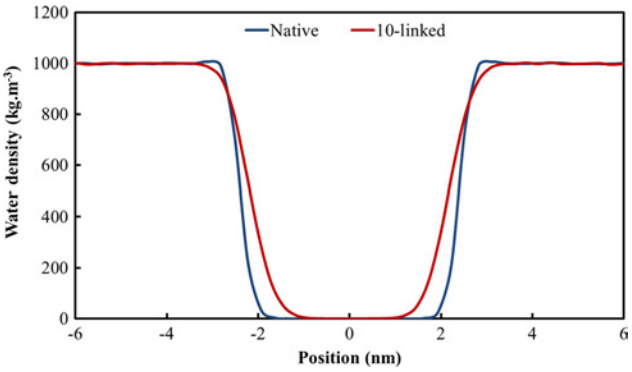

FIGURE 4 Water density across the SC along the bilayer normal, in a structure containing no CL ceramides versus a structure consisting of 44% of 10-linked ceramides (shown as representative example of a CL SC system). CL, cross-linked; SC, stratum corneum

artifact cannot be avoided in our analysis, but we do believe that this is the best analysis tool available.

The correlation between the increase in void size in the SC and the permeability of water molecules is illustrated in Figure 4, by looking at the distribution of water molecules across the structure when introducing CL ceramides into the SC. Indeed, this figure shows that after polymerization, the tendency of water molecules to populate the bilayer interior increases. Although no water molecules are able to reach the center of the membrane (in agreement with the absence of pore formation in our simulations), this increase in water permeability can still allow for an increase of the permeability of drugs, for example, in the case of the presence of an electric field over the SC structure (present in, e.g., floating-electrode dielectric-barrier discharges).[33]

Figure 5 shows a snapshot of one of the SC structures investigated, illustrating the pores (visualized using the VMD program[34]). The seemingly rough edges of the pores shown in Figure 5 originate from the method used, in which cubic cells are used to identify voids (see discussion above). Note that only a slice (along the *xz*-plane) is displayed in Figure 5, to be able to visualize these voids.

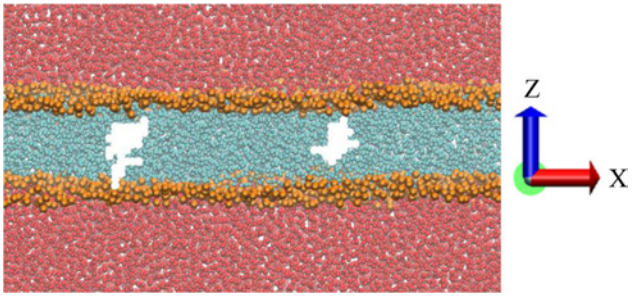

FIGURE 5 Front view of a ceramide bilayer system. The water molecules above and below the bilayer are depicted as red spheres, the ceramide head group regions are depicted as orange spheres and the lipid tails in cyan. The two biggest voids observed in this system (biggest clusters of free grid cells) are depicted in white. In this system (DOP = 10, 44% of CL ceramides), around 10% of the entire membrane is void. CL, cross-linked; DOP, degree of polymerization

4 | CONCLUSION

We have performed coarse-grained MD simulations in search of the mechanism behind CAP-enhanced TDD. The hypothesis put forward is that lipid tail oxidation, induced by plasma-generated ROS, leads to the formation of cross-linkages between neighboring ceramides. This, in turn, leads to the generation of nanopores, which facilitate the diffusion of drug molecules through skin tissue, as observed experimentally. Our MD simulations reveal that CL of the ceramides indeed induces the creation of voids in the SC structure, which leads to an increase of the permeability of water molecules, indicating that this process could facilitate the diffusion of drugs. Furthermore, our results predict that there will be an optimal treatment time to achieve maximum enhancement of the SC permeability, which, experimentally, will depend on the exact composition of the SC, as well as on the plasma source used. Overall, our results indicate that the induction of ceramide CL can be an explanation for the experimentally observed ability of CAP to enhance TDD.

ACKNOWLEDGMENTS

We acknowledge the financial support from the Research Foundation-Flanders (FWO) (Grant No.: 11U5416N). The computational resources and services used in this study were provided by the VSC (Flemish Supercomputer Center), funded by the FWO and the Flemish Government-department EWI.

ORCID

Jonas Van der Paal http://orcid.org/0000-0002-6885-8236

REFERENCES

[1] M. R. Prausnitz, R. Langer, *Nat. Biotechnol.* **2008**, *26*, 1261.
[2] M. A. Moses, H. Brem, R. Langer, *Cancer Cell* **2003**, *4*, 337.
[3] M. R. Prausnitz, S. Mitragotri, R. Langer, *Nat. Rev. Drug. Discov.* **2004**, *3*, 115.
[4] H. Marwah, T. Garg, A. K. Goyal, G. Rath, *Drug Deliv.* **2016**, *23*, 564.

[5] I. Iwai, H. Han, L. Hollander, S. Svensson, L.-G. Öfverstedt, J. Anwar, J. Brewer, M. Bloksgaard, *J. Invest. Dermatol.* **2012**, *132*, 2215.
[6] B. Forslind, M. Lindberg, in *Skin, hair and nails*, 1st ed., CRC Press, Boca Raton, FL **2003**.
[7] J. A. Bouwstra, F. E. R. Dubbelaar, G. S. Gooris, M. Ponec, *Acta Derm.-Venereol.* **2000**, *208*, 23.
[8] S. Mitragotri, *Adv. Drug Deliv. Rev.* **2013**, *65*, 100.
[9] O. Lademann, H. Richter, M. C. Meinke, A. Patzelt, A. Kramer, P. Hinz, K. D. Weltmann, B. Hartmann, S. Koch, *Exp. Dermatol.* **2011**, *20*, 488.
[10] K. Shimizu, K. Hayashida, M. Blajan, *Biointerphases* **2015**, *10*, 029517.
[11] K. Shimizu, N. A. Tran, K. Hayashida, M. Blajan, *J. Phys. D: Appl. Phys.* **2016**, *49*, 315201.
[12] M. Gelker, C. C. Müller-Goymann, W. Viöl, *Clin. Plasma Med.* **2018**, *9*, 34.
[13] A. Lehmann, F. Pietag, T. Arnold, *Clin. Plasma Med.* **2017**, *7*, 16.
[14] A. Reis, C. M. Spickett, *Biochim. Biophys. Acta* **2012**, *1818*, 2374.
[15] A. Catalá, *Biochem. Biophys. Res. Commun.* **2010**, *399*, 318.
[16] H. S. El-Beltagi, H. I. Mohamed, *Not. Bot. Horti Agrobot.* **2013**, *41*, 44.
[17] G. Barrera, L. Peroxidation, *Int. Scholarly Res. Not. Oncol.* **2012**, 137289.
[18] T. Melo, E. Maciel, M. M. Oliveira, P. Domingues, M. R. M. Domingues, *Eur. J. Lipid Sci. Technol.* **2012**, *114*, 726.
[19] W. J. Muizebelt, M. W. F. Nielen, *J. Mass Spectrom.* **1996**, *31*, 545.
[20] H. W. Gardner, *Free Radic. Biol. Med.* **1989**, *7*, 65.
[21] M. A. R. Meier, J. O. Metzger, U. S. Schubert, *Chem. Soc. Rev.* **2007**, *36*, 1788.
[22] F. Seniha Güner, Y. Yağcı, A. Tuncer Erciyes, *Prog. Polym. Sci.* **2006**, *31*, 633.
[23] S. E. Feller, *Curr. Opin. Colloid Interface Sci.* **2000**, *5*, 217.
[24] J. Van Der Paal, E. C. Neyts, C. C. W. Verlackt, A. Bogaerts, *Chem. Sci.* **2015**, *7*, 489.
[25] J. Van der Paal, C. Verheyen, E. C. Neyts, A. Bogaerts, *Sci. Rep.* **2017**, *7*, 39526.
[26] J. M. Jungersted, L. I. Hellgren, J. K. Høgh, T. Drachmann, G. B. E. Jemec, T. Agner, *Acta Derm.-Venereol.* **2010**, *90*, 350.
[27] L. Martínez, R. Andrade, E. G. Birgin, J. M. Martínez, *J. Comput. Chem.* **2009**, *30*, 2157.
[28] G. Bussi, D. Donadio, M. Parrinello, *J. Chem. Phys.* **2007**, *126*, 014101.
[29] M. Parrinello, A. Rahman, *J. Appl. Phys.* **1981**, *52*, 7182.
[30] S. J. Marrink, H. J. Risselada, S. Yefimov, D. P. Tieleman, A. H. De Vries, *J. Phys. Chem. B* **2007**, *111*, 7812.
[31] A. Bogaerts, N. Khosravian, J. Van der Paal, C. C. W. Verlackt, M. Yusupov, B. Kamaraj, E. C. Neyts, *J. Phys. D: Appl. Phys.* **2016**, *49*, 054002.
[32] P. Sane, E. Salonen, E. Falck, J. Repakova, F. Tuomisto, J. M. Holopainen, I. Vattulainen, *J. Phys. Chem. Lett. B* **2009**, *113*, 1810.
[33] M. Yusupov, J. Van der Paal, E. C. Neyts, A. Bogaerts, *Biochim. Biophys. Acta, Gen. Subj.* **2017**, *1861*, 839.
[34] W. Humphrey, A. Dalke, K. Schulten, *J. Mol. Graph.* **1996**, *14*, 33.

How to cite this article: Van der Paal J, Fridman G, Bogaerts A. Ceramide cross-linking leads to pore formation: potential mechanism behind CAP enhancement of transdermal drug delivery. *Plasma Process Polym*. 2019;e1900122. https://doi.org/10.1002/ppap.201900122

APPENDIX A: CROSS-LINKED CERAMIDES TOPOLOGY

The data shown below, which is included in the topology file, lists the topology of oligoceramides containing two or three cross-linked ceramides. Chains containing a higher number of linked ceramides were constructed analogously

```
[moleculetype]
; molname       nrexcl
  PNC2           1                              ;;; CERAMIDE DIMER

[atoms]
; id    type    resnr   residu  atom    cgnr    charge
   1    P1       1      PNC2    AM1      1      0
   2    P5       1      PNC2    AM2      2      0
   3    C3       1      PNC2    T1A      3      0
   4    C1       1      PNC2    C2A      4      0
   5    C1       1      PNC2    C3A      5      0
   6    C1       1      PNC2    C1B      6      0
   7    C1       1      PNC2    C2B      7      0
   8    C1       1      PNC2    C3B      8      0
   9    C3       1      PNC2    D4B      9      0
  10    C1       1      PNC2    C5B     10      0
  11    C1       1      PNC2    C6B     11      0

  12    P1       1      PNC2    AM1     12      0
  13    P5       1      PNC2    AM2     13      0
  14    C3       1      PNC2    T1A     14      0
  15    C1       1      PNC2    C2A     15      0
  16    C1       1      PNC2    C3A     16      0
  17    C1       1      PNC2    C1B     17      0
  18    C1       1      PNC2    C2B     18      0
  19    C1       1      PNC2    C3B     19      0
  20    C3       1      PNC2    D4B     20      0
  21    C1       1      PNC2    C5B     21      0
  22    C1       1      PNC2    C6B     22      0

[bonds]
;  i   j        funct   length  force.c.
   1   2        1       0.37    1250
   1   3        1       0.47    1250
   3   4        1       0.47    1250
   4   5        1       0.47    1250
   2   6        1       0.47    1250
   6   7        1       0.47    1250
   7   8        1       0.47    1250
   8   9        1       0.47    1250
   9  10        1       0.47    1250
  10  11        1       0.47    1250

  12  13        1       0.37    1250
  12  14        1       0.47    1250
  14  15        1       0.47    1250
  15  16        1       0.47    1250
  13  17        1       0.47    1250
  17  18        1       0.47    1250
  18  19        1       0.47    1250
  19  20        1       0.47    1250
  20  21        1       0.47    1250
  21  22        1       0.47    1250

   8  19        1       0.47    1250        ;;; CROSS-LINKING BOND

[angles]
;  i   j   k     funct   angle   force.c.
   1   3   4     2       180.0   45.0
   3   4   5     2       180.0   25.0
   2   6   7     2       180.0   25.0
   6   7   8     2       180.0   25.0
   7   8   9     2       180.0   25.0
   8   9  10     2       120.0   45.0
```

```
   9 10 11      2       180.0   25.0

  12 14 15      2       180.0   45.0
  14 15 16      2       180.0   25.0
  13 17 18      2       180.0   25.0
  17 18 19      2       180.0   25.0
  18 19 20      2       180.0   25.0
  19 20 21      2       120.0   45.0
  20 21 22      2       180.0   25.0

   7  8 19      2       120.0   45.0
   9  8 19      2       120.0   45.0
   8 19 20      2       120.0   45.0
   8 19 18      2       120.0   45.0


[moleculetype]
; molname       nrexcl
  PNC3          1                               ;;; CERAMIDE TRIMER

[atoms]
; id    type    resnr   residu  atom    cgnr    charge
   1    P1       1      PNC3    AM1      1      0
   2    P5       1      PNC3    AM2      2      0
   3    C3       1      PNC3    T1A      3      0
   4    C1       1      PNC3    C2A      4      0
   5    C1       1      PNC3    C3A      5      0
   6    C1       1      PNC3    C1B      6      0
   7    C1       1      PNC3    C2B      7      0
   8    C1       1      PNC3    C3B      8      0
   9    C3       1      PNC3    D4B      9      0
  10    C1       1      PNC3    C5B     10      0
  11    C1       1      PNC3    C6B     11      0

  12    P1       1      PNC3    AM1     12      0
  13    P5       1      PNC3    AM2     13      0
  14    C3       1      PNC3    T1A     14      0
  15    C1       1      PNC3    C2A     15      0
  16    C1       1      PNC3    C3A     16      0
  17    C1       1      PNC3    C1B     17      0
  18    C1       1      PNC3    C2B     18      0
  19    C1       1      PNC3    C3B     19      0
  20    C3       1      PNC3    D4B     20      0
  21    C1       1      PNC3    C5B     21      0
  22    C1       1      PNC3    C6B     22      0

  23    P1       1      PNC3    AM1     23      0
  24    P5       1      PNC3    AM2     24      0
  25    C3       1      PNC3    T1A     25      0
  26    C1       1      PNC3    C2A     26      0
  27    C1       1      PNC3    C3A     27      0
  28    C1       1      PNC3    C1B     28      0
  29    C1       1      PNC3    C2B     29      0
  30    C1       1      PNC3    C3B     30      0
  31    C3       1      PNC3    D4B     31      0
  32    C1       1      PNC3    C5B     32      0
  33    C1       1      PNC3    C6B     33      0


[bonds]
;  i   j        funct   length  force.c.
   1   2        1       0.37    1250
   1   3        1       0.47    1250
   3   4        1       0.47    1250
```

```
  4  5          1       0.47    1250
  2  6          1       0.47    1250
  6  7          1       0.47    1250
  7  8          1       0.47    1250
  8  9          1       0.47    1250
  9 10          1       0.47    1250
 10 11          1       0.47    1250


 12 13          1       0.37    1250
 12 14          1       0.47    1250
 14 15          1       0.47    1250
 15 16          1       0.47    1250
 13 17          1       0.47    1250
 17 18          1       0.47    1250
 18 19          1       0.47    1250
 19 20          1       0.47    1250
 20 21          1       0.47    1250
 21 22          1       0.47    1250

  8 19          1       0.47    1250       ;;; CROSS-LINKING BOND

 23 24          1       0.37    1250
 23 25          1       0.47    1250
 25 26          1       0.47    1250
 26 27          1       0.47    1250
 24 28          1       0.47    1250
 28 29          1       0.47    1250
 29 30          1       0.47    1250
 30 31          1       0.47    1250
 31 32          1       0.47    1250
 32 33          1       0.47    1250

 15 26          1       0.47    1250       ;;; CROSS-LINKING BOND


[angles]
;  i  j  k      funct   angle   force.c.
   1  3  4      2       180.0   45.0
   3  4  5      2       180.0   25.0
   2  6  7      2       180.0   25.0
   6  7  8      2       180.0   25.0
   7  8  9      2       180.0   25.0
   8  9 10      2       120.0   45.0
   9 10 11      2       180.0   25.0

 12 14 15       2       180.0   45.0
 14 15 16       2       180.0   25.0
 13 17 18       2       180.0   25.0
 17 18 19       2       180.0   25.0
 18 19 20       2       180.0   25.0
 19 20 21       2       120.0   45.0
 20 21 22       2       180.0   25.0

  7  8 19       2       120.0   45.0       ;;; CROSS-LINKING ANGLE
  9  8 19       2       120.0   45.0       ;;; CROSS-LINKING ANGLE
  8 19 20       2       120.0   45.0       ;;; CROSS-LINKING ANGLE
  8 19 18       2       120.0   45.0       ;;; CROSS-LINKING ANGLE

 23 25 26       2       180.0   45.0
 25 26 27       2       180.0   25.0
 24 28 29       2       180.0   25.0
 28 29 30       2       180.0   25.0
 29 30 31       2       180.0   25.0
```

```
30 31 32        2       120.0   45.0
31 32 33        2       180.0   25.0

14 15 26        2       120.0   45.0        ;;; CROSS-LINKING ANGLE
15 26 27        2       120.0   45.0        ;;; CROSS-LINKING ANGLE
16 15 26        2       120.0   45.0        ;;; CROSS-LINKING ANGLE
15 26 25        2       120.0   45.0        ;;; CROSS-LINKING ANGLE
```